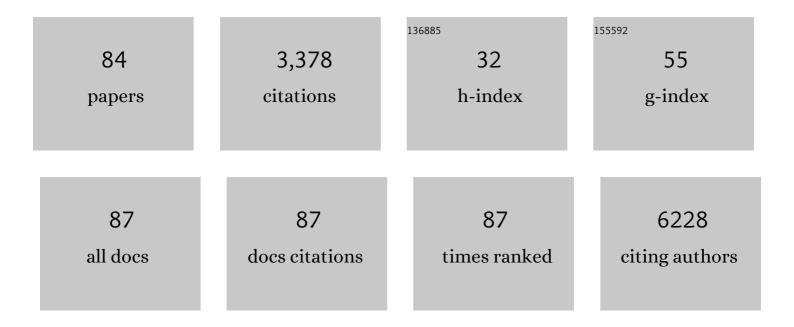
Thomas Abraham

List of Publications by Year in descending order

Source: https://exaly.com/author-pdf/7540222/publications.pdf Version: 2024-02-01



#	Article	IF	CITATIONS
1	Contribution of Intimal Smooth Muscle Cells to Cholesterol Accumulation and Macrophage-Like Cells in Human Atherosclerosis. Circulation, 2014, 129, 1551-1559.	1.6	493
2	An autophagy assay reveals the ESCRT-III component CHMP2A as a regulator of phagophore closure. Nature Communications, 2018, 9, 2855.	5.8	240
3	TIMP2 Deficiency Accelerates Adverse Post–Myocardial Infarction Remodeling Because of Enhanced MT1-MMP Activity Despite Lack of MMP2 Activation. Circulation Research, 2010, 106, 796-808.	2.0	140
4	miR-33a Modulates ABCA1 Expression, Cholesterol Accumulation, and Insulin Secretion in Pancreatic Islets. Diabetes, 2012, 61, 653-658.	0.3	122
5	Inducible reprogramming of human T cells into Treg cells by a conditionally active form of FOXP3. European Journal of Immunology, 2008, 38, 3282-3289.	1.6	91
6	A Splice Variant of the Human Ion Channel TRPM2 Modulates Neuroblastoma Tumor Growth through Hypoxia-inducible Factor (HIF)-1/2α. Journal of Biological Chemistry, 2014, 289, 36284-36302.	1.6	82
7	Tumor-promoting effects of pancreatic cancer cell exosomes on THP-1-derived macrophages. PLoS ONE, 2018, 13, e0206759.	1.1	81
8	Direct Measurements of Interactions between Hydrophobically Anchored Strongly Charged Polyelectrolyte Brushes. Langmuir, 2000, 16, 4286-4292.	1.6	78
9	Macrophage-Tumor Cell Fusions from Peripheral Blood of Melanoma Patients. PLoS ONE, 2015, 10, e0134320.	1.1	76
10	Mechanical force modulates scleraxis expression in bioartificial tendons. Journal of Musculoskeletal Neuronal Interactions, 2011, 11, 124-32.	0.1	76
11	Extracellular matrix remodeling of lung alveolar walls in three dimensional space identified using second harmonic generation and multiphoton excitation fluorescence. Journal of Structural Biology, 2010, 171, 189-196.	1.3	75
12	VPS37A directs ESCRT recruitment for phagophore closure. Journal of Cell Biology, 2019, 218, 3336-3354.	2.3	74
13	Early activation of matrix metalloproteinases underlies the exacerbated systolic and diastolic dysfunction in mice lacking TIMP3 following myocardial infarction. American Journal of Physiology - Heart and Circulatory Physiology, 2010, 299, H1012-H1023.	1.5	73
14	Isothermal Titration Calorimetry Studies of the Binding of a Rationally Designed Analogue of the Antimicrobial Peptide Gramicidin S to Phospholipid Bilayer Membranes. Biochemistry, 2005, 44, 2103-2112.	1.2	63
15	Asphalteneâ~'Silica Interactions in Aqueous Solutions:Â Direct Force Measurements Combined with Electrokinetic Studies. Industrial & Engineering Chemistry Research, 2002, 41, 2170-2177.	1.8	60
16	Depletion of the Human Ion Channel TRPM2 in Neuroblastoma Demonstrates Its Key Role in Cell Survival through Modulation of Mitochondrial Reactive Oxygen Species and Bioenergetics. Journal of Biological Chemistry, 2016, 291, 24449-24464.	1.6	58
17	Granzyme B contributes to extracellular matrix remodeling and skin aging in apolipoprotein E knockout mice. Experimental Gerontology, 2011, 46, 489-499.	1.2	57
18	Serpina3n attenuates granzyme B-mediated decorin cleavage and rupture in a murine model of aortic aneurysm. Cell Death and Disease, 2011, 2, e209-e209.	2.7	57

#	Article	IF	CITATIONS
19	<i>Scleraxis</i> expression is coordinately regulated in a murine model of patellar tendon injury. Journal of Orthopaedic Research, 2011, 29, 289-296.	1.2	54
20	B Cell–Intrinsic CD84 and Ly108 Maintain Germinal Center B Cell Tolerance. Journal of Immunology, 2015, 194, 4130-4143.	0.4	53
21	Humans with inherited TÂcell CD28 deficiency are susceptible to skin papillomaviruses but are otherwise healthy. Cell, 2021, 184, 3812-3828.e30.	13.5	53
22	"Stealth dissemination" of macrophage-tumor cell fusions cultured from blood of patients with pancreatic ductal adenocarcinoma. PLoS ONE, 2017, 12, e0184451.	1.1	51
23	Neutron Diffraction Study ofPseudomonasaeruginosaLipopolysaccharide Bilayers. Journal of Physical Chemistry B, 2007, 111, 2477-2483.	1.2	48
24	Isothermal Titration Calorimetry Studies of the Binding of the Antimicrobial Peptide Gramicidin S to Phospholipid Bilayer Membranesâ€. Biochemistry, 2005, 44, 11279-11285.	1.2	46
25	Increased mast cell numbers in a calcaneal tendon overuse model. Scandinavian Journal of Medicine and Science in Sports, 2013, 23, e353-60.	1.3	46
26	Adsorption Kinetics of a Hydrophobicâ 'Hydrophilic Diblock Polyelectrolyte at the Solidâ 'Aqueous Solution Interface:Â A Slow Birth and Fast Growth Process. Macromolecules, 2000, 33, 6051-6059.	2.2	42
27	The Bif-1-Dynamin 2 membrane fission machinery regulates Atg9-containing vesicle generation at the Rab11-positive reservoirs. Oncotarget, 2016, 7, 20855-20868.	0.8	42
28	Extracellular vesicle-dependent effect of RNA-binding protein IGF2BP1 on melanoma metastasis. Oncogene, 2019, 38, 4182-4196.	2.6	41
29	Polyelectrolyte-Mediated Interaction between Similarly Charged Surfaces:Â Role of Divalent Counter Ions in Tuning Surface Forces. Langmuir, 2001, 17, 8321-8327.	1.6	40
30	Glycolipid based cubic nanoparticles: preparation and structural aspects. Colloids and Surfaces B: Biointerfaces, 2004, 35, 107-118.	2.5	38
31	Polymer-Dispersed Bicontinuous Cubic Glycolipid Nanoparticles. Biotechnology Progress, 2008, 21, 255-262.	1.3	38
32	Context-dependent activation of SIRT3 is necessary for anchorage-independent survival and metastasis of ovarian cancer cells. Oncogene, 2020, 39, 1619-1633.	2.6	37
33	A Cholecystokinin B Receptor-Specific DNA Aptamer for Targeting Pancreatic Ductal Adenocarcinoma. Nucleic Acid Therapeutics, 2017, 27, 23-35.	2.0	34
34	Collagen matrix remodeling in 3-dimensional cellular space resolved using second harmonic generation and multiphoton excitation fluorescence. Journal of Structural Biology, 2010, 169, 36-44.	1.3	33
35	Second harmonic generation analysis of early Achilles tendinosis in response to in vivo mechanical loading. BMC Musculoskeletal Disorders, 2011, 12, 26.	0.8	33
36	ERK MAP kinase-activated Arf6 trafficking directs coxsackievirus type B3 into an unproductive compartment during virus host-cell entry. Journal of General Virology, 2009, 90, 854-862.	1.3	32

#	Article	IF	CITATIONS
37	Versican V1 Overexpression Induces a Myofibroblast-Like Phenotype in Cultured Fibroblasts. PLoS ONE, 2015, 10, e0133056.	1.1	31
38	Monolayer Film Behavior of Lipopolysaccharide from Pseudomonas aeruginosa at the Airâ^'Water Interface. Biomacromolecules, 2008, 9, 2799-2804.	2.6	29
39	Structure–activity relationships of the antimicrobial peptide gramicidin S and its analogs: Aqueous solubility, self-association, conformation, antimicrobial activity and interaction with model lipid membranes. Biochimica Et Biophysica Acta - Biomembranes, 2014, 1838, 1420-1429.	1.4	29
40	Podocalyxin Regulates Murine Lung Vascular Permeability by Altering Endothelial Cell Adhesion. PLoS ONE, 2014, 9, e108881.	1.1	26
41	Vitronectin Expression in the Airways of Subjects with Asthma and Chronic Obstructive Pulmonary Disease. PLoS ONE, 2015, 10, e0119717.	1.1	26
42	Minimally invasive multiphoton and harmonic generation imaging of extracellular matrix structures in lung airway and related diseases. Pulmonary Pharmacology and Therapeutics, 2011, 24, 487-496.	1.1	25
43	Role of polyelectrolyte charge density in tuning colloidal forces. AICHE Journal, 2004, 50, 2613-2626.	1.8	24
44	Quantitative assessment of forward and backward second harmonic three dimensional images of collagen Type I matrix remodeling in a stimulated cellular environment. Journal of Structural Biology, 2012, 180, 17-25.	1.3	24
45	A peptide derived from melanotransferrin delivers a protein-based interleukin 1 receptor antagonist across the BBB and ameliorates neuropathic pain in a preclinical model. Journal of Cerebral Blood Flow and Metabolism, 2019, 39, 2074-2088.	2.4	22
46	Aberrant structure of fibrillar collagen and elevated levels of advanced glycation end products typify delayed fracture healing in the diet-induced obesity mouse model. Bone, 2020, 137, 115436.	1.4	21
47	Effects of divalent salt on adsorption kinetics of a hydrophobically modified polyelectrolyte at the neutral surface–aqueous solution interface. Polymer, 2002, 43, 849-855.	1.8	19
48	The relationship between the binding to and permeabilization of phospholipid bilayer membranes by GS14dK4, a designed analog of the antimicrobial peptide gramicidin S. Biochimica Et Biophysica Acta - Biomembranes, 2007, 1768, 2089-2098.	1.4	19
49	Functional effects of protein kinases and peroxynitrite on cardiac carnitine palmitoyltransferase-1 in isolated mitochondria. Molecular and Cellular Biochemistry, 2010, 337, 223-237.	1.4	19
50	Cryo-imaging of Inflated Frozen Human Lung Sections at -60°C using Multiphoton and Harmonic Generation Microscopy. Microscopy and Microanalysis, 2014, 20, 1348-1349.	0.2	19
51	Adhesion forces between functionalized probes and hydrophilic silica surfaces. Journal of Adhesion Science and Technology, 2005, 19, 149-163.	1.4	18
52	Proteomic identification of dysferlin-interacting protein complexes in human vascular endothelium. Biochemical and Biophysical Research Communications, 2011, 415, 263-269.	1.0	18
53	Proteinase inhibitor 9 is reduced in human atherosclerotic lesion development. Cardiovascular Pathology, 2012, 21, 28-38.	0.7	18
54	SH3GLB2/endophilin B2 regulates lung homeostasis and recovery from severe influenza A virus infection. Scientific Reports, 2017, 7, 7262.	1.6	17

#	Article	IF	CITATIONS
55	Versican localizes to the nucleus in proliferating mesenchymal cells. Cardiovascular Pathology, 2015, 24, 368-374.	0.7	16
56	Simple Experimental Methods for Determining the Apparent Focal Shift in a Microscope System. PLoS ONE, 2015, 10, e0134616.	1.1	16
57	Minimally invasive imaging method based on second harmonic generation and multiphoton excitation fluorescence in translational respiratory research. Respirology, 2011, 16, 22-33.	1.3	15
58	A novel dual inhibitor of microtubule and Bruton's tyrosine kinase inhibits survival of multiple myeloma and osteoclastogenesis. Experimental Hematology, 2017, 53, 31-42.	0.2	15
59	Second harmonic generation microscopy differentiates collagen type I and type III in diseased lung tissues. Proceedings of SPIE, 2012, , .	0.8	13
60	Liposomal delivery of ferritin heavy chain 1 (FTH1) siRNA in patient xenograft derived glioblastoma initiating cells suggests different sensitivities to radiation and distinct survival mechanisms. PLoS ONE, 2019, 14, e0221952.	1.1	13
61	A Nanomule Peptide Carrier Delivers siRNA Across the Intact Blood-Brain Barrier to Attenuate Ischemic Stroke. Frontiers in Molecular Biosciences, 2021, 8, 611367.	1.6	13
62	Sodium cromolyn reduces expression of CTGF, ADAMTS1, and TIMP3 and modulates postâ€ i njury patellar tendon morphology. Journal of Orthopaedic Research, 2011, 29, 678-683.	1.2	12
63	Domain Interaction Studies of Herpes Simplex Virus 1 Tegument Protein UL16 Reveal Its Interaction with Mitochondria. Journal of Virology, 2017, 91, .	1.5	12
64	Effective encapsulation and biological activity of phosphorylated chemotherapeutics in calcium phosphosilicate nanoparticles for the treatment of pancreatic cancer. Nanomedicine: Nanotechnology, Biology, and Medicine, 2017, 13, 2313-2324.	1.7	11
65	Localization of DNA and RNA in Eosinophil Secretory Granules. International Archives of Allergy and Immunology, 2010, 152, 12-27.	0.9	10
66	Deconvolution and chromatic aberration corrections in quantifying colocalization of a transcription factor in three-dimensional cellular space. Micron, 2010, 41, 633-640.	1.1	9
67	PIGN gene expression aberration is associated with genomic instability and leukemic progression in acute myeloid leukemia with myelodysplastic features. Oncotarget, 2017, 8, 29887-29905.	0.8	9
68	ADAM15 is required for optimal collagen cross-linking and scar formation following myocardial infarction. Matrix Biology, 2022, 105, 127-143.	1.5	9
69	Structural changes in the collagen network of joint tissues in late stages of murine OA. Scientific Reports, 2022, 12, .	1.6	8
70	Interactions of partially screened polyelectrolyte layers with oppositely charged surfactant in confined environment. Colloids and Surfaces A: Physicochemical and Engineering Aspects, 2001, 180, 103-110.	2.3	7
71	Aptamer-Targeted Calcium Phosphosilicate Nanoparticles for Effective Imaging of Pancreatic and Prostate Cancer. International Journal of Nanomedicine, 2021, Volume 16, 2297-2309.	3.3	7

Neutron Diffraction Study of Pseudomonas aeruginosa Lipopolysaccharide Bilayers. , 0, , .

7

#	Article	IF	CITATIONS
73	Discovery of a Highly Conserved Peptide in the Iron Transporter Melanotransferrin that Traverses an Intact Blood Brain Barrier and Localizes in Neural Cells. Frontiers in Neuroscience, 2021, 15, 596976.	1.4	5
74	Response to Letter Regarding Article, "Contribution of Intimal Smooth Muscle Cells to Cholesterol Accumulation and Macrophage-Like Cells in Human Atherosclerosis― Circulation, 2015, 131, e25.	1.6	3
75	PIGN spatiotemporally regulates the spindle assembly checkpoint proteins in leukemia transformation and progression. Scientific Reports, 2021, 11, 19022.	1.6	3
76	Imaging of collagen matrix remodeling in three-dimensional space using second harmonic generation and two photon excitation fluorescence. , 2009, , .		1
77	Quantifying colocalization of a conditionally active transcription factor FOXP3 in three-dimensional cellular space. Proceedings of SPIE, 2009, , .	0.8	0
78	Lung alveolar wall disruption in three-dimensional space identified using second-harmonic generation and multiphoton excitation fluorescence. , 2010, , .		0
79	Second harmonic generation imaging of collagen matrix remodeling in a stimulated 3D cellular environment: forward versus backward detection. , 2011, , .		0
80	Multiphoton microscopy based cryo-imaging of inflated frozen human lung sections at -60°C in healthy and COPD lungs. Proceedings of SPIE, 2013, , .	0.8	0
81	Bio-distribution of near infrared imaging agent loaded targeted drug nanoparticle carriers in highly fibrotic pancreatic tumor determined using multiphoton and harmonic generation imaging. , 2018, , .		0
82	Pign Suppresses CIN and Leukemia Progression Via Regulation of the Spindle Assembly Checkpoint. Blood, 2018, 132, 2792-2792.	0.6	0
83	Multiphoton and harmonic generation imaging methods enable direct visualization of drug nanoparticle carriers in conjunction with vasculature in fibrotic prostate tumor mouse model. , 2019, , .		0
84	Educating and training biomedical researchers in biophotonics and advanced light microscopy methods. , 2019, , .		0